International Journal of Human-Computer Studies 140 (2020) 102432

Contents lists available at ScienceDirect

International Journal of Human-Computer Studies

journal homepage: www.elsevier.com/locate/ijhcs

Effect of target distance on controllability for myocontrol

Cassie N. Borish[a,*], Matteo Bertucco[b], Terence D. Sanger[c]

[a] Department of Biomedical Engineering, University of Southern California, Los Angeles, CA, 90089 USA
[b] Department of Neurosciences, Biomedicine and Movement Sciences, University of Verona, Verona, 37131 Italy
[c] School of Engineering, University of California, Irvine, CA, 92697 USA

ARTICLE INFO

Keywords:
Fitts's law
Electromyography
Myoelectric control
Motor unit variability

ABSTRACT

Myocontrol holds great promise because it has the potential to provide flexible and accurate prosthetic control that approaches the quality of normal movement. Speed and accuracy are important factors to consider when applying myoelectric signals to external devices. Fitts's law can be used to assess the speed-accuracy trade-off. We hypothesized that speed is affected not only by accuracy as prescribed by Fitts's law, but also by target distances independent of target size. A total of 12 healthy adult subjects were studied. Subjects controlled the vertical movement of a computer cursor by contracting their dominant first dorsal interosseus muscle to reach targets as quickly as possible. We manipulated twenty-five different target distances in order to obtain five indices of difficulty, as defined by Fitts's law, combined with five target widths. We tested the relationship between movement time and the index of difficulty as predicted by Fitts's law among different combinations of target distance and widths. Results showed a significant linear regression for all conditions, with the exception of a significantly longer movement time than predicted for targets close to the start point. Movements to these targets showed significantly higher relative variance during stabilization, higher overshoot, and lower success. Therefore, we found that with comparable index of difficulty, small distance movements had a higher variability, slower movement, and higher rates of error compared to larger distance movements. Our results are consistent with our hypothesis that low muscle activation required for short distances results in higher variability and low controllability in reaching the target as required by the task demand. Neurophysiological mechanisms underlying the violation of the Fitts's law relationship are discussed. These results have significance for myocontrol applications, and we suggest that such applications require control signals with sufficient recruitment to reduce variability at lower levels of muscle activation.

1. Introduction

Myocontrol, the control of external devices using electromyographic (*EMG*) signals, holds great promise because it has the potential to provide flexible and accurate control that approaches the quality of normal movement. Myoelectrically controlled limb prosthetics have long been in development and have become an established technology (Childress, 1985; Farina and Amsuss, 2016; Smith et al., 2016). More recently, the use of myocontrol has extended beyond control of limb prosthetics. Myoelectric signals can also be used for biofeedback (Bloom et al., 2010; Williams and Kirsch, 2009; Young et al., 2011b,a, Young et al., 2014) and functional electrical stimulation (Seifert and Fuglevand, 2002) for rehabilitation, as well as the control of other external devices such as exoskeletons (Ambrosini et al., 2014) and speech synthesizers (Niu et al., 2015). Due to the increasing prevalence of myocontrol, there is a need to understand its boundaries of controllability and how to optimize parameters to provide the best possible control.

There still exist many challenges to using *EMG* signals for control. The most straightforward approach to estimate motor intent is by estimating the intensity of the *EMG* signal. The clarity of the signal itself can be influenced by electrode placement, how the signal is filtered, and the range of *EMG* activation. The signal is generally normalized to address potential differences in electrode placement (Staudenmann et al., 2010). While it is common for the *EMG* signal to be linearly filtered to remove noise, it has been shown that a non-linear Bayesian filter can better estimate rapid changes in the signal (Sanger, 2007). It has also been shown that Bayesian filtered *EMG* provides more accurate simultaneous and proportional myocontrol (Hofmann et al., 2016; Borish et al., 2018).

How *EMG* activation levels impact the controllability of myocontrol has not been thoroughly investigated. While the upper threshold for

* Corresponding author. Tel.: +16028828173
E-mail addresses: cassieborish@gmail.com (C.N. Borish), matteo.bertucco@univr.it (M. Bertucco), terry@sangerlab.net (T.D. Sanger).

https://doi.org/10.1016/j.ijhcs.2020.102432
Received 24 January 2018; Received in revised form 26 November 2019; Accepted 21 March 2020
Available online 06 April 2020
1071-5819/ © 2020 Elsevier Ltd. All rights reserved.

myocontrol activation is primarily dictated by fatigue, the lower threshold of activation has not been explored.

Speed and accuracy are important factors to consider when applying myoelectric signals to external devices. Speed provides subjects a more natural and intuitive interface so that the external device more closely resembles an extension of their own limb. Accuracy is necessary for users to meet task demands. However, in motor control and human-computer interaction there is a trade-off between speed and accuracy. The more accurate the task to be accomplished, the longer it takes and vice versa (Plamondon and Alimi, 1997).

The most well-known mathematical formulation of the trade-off between speed and accuracy was introduced by Fitts (Fitts, 1954), who showed that the movement time (*MT*) to reach a target increases with movement distance (*D*), and decreases as target size increases (*W*), such that $MT = a + b \log_2 (2D/W)$, wherein a and b are empirical constants (the intercept and the slope of the regression line, respectively), and $\log_2 (2D/W)$ represents the index of difficulty (*ID*). This relationship predicts that at a constant $2D/W$ ratio, *MT* will remain unchanged. Hence, *MT* is directly proportional to the *ID*, which may have the same value for different combinations of movement parameters *D* and *W*. Fitts derived his work making an analogy of the human motor system with the well-known information theory by Shannon (1948). From the Fitts's law model, the inverse of the slope of the regression line ($1/b$) is defined as the Index of Performance (IP), since the higher its value, the less *MT* is affected by increases in task difficulty. In accordance with the channel capacity theorem (Shannon, 1948) the IP can be interpreted as the bandwidth of the motor control system for a given task.

Given its direct linkage with the information theory and channel capacity theorem, Fitts's law has been used extensively in the field of human-computer interfaces (HCI) as a tool to characterize the bandwidth of interfaces, such as mice or trackpads, which can be explained as the information rate for a given device (MacKenzie, 1992; Soukoreff and MacKenzie, 2004). Therefore, Fitts's law proves to be also a valuable tool to assess controllability of myocontrol interfaces (Scheme and Englehart, 2013; Kamavuako et al., 2014; Gusman et al., 2017; Vujaklija et al., 2018).

Fitts's law has been explained under the hypothesis of signal-dependent noise, if random and uncontrollable noise in the motor system increases as the magnitude of the signal increases, then increasing success can only be achieved by decreasing the magnitude of the signal or increasing the target width (Schmidt et al.,1979; Harris and Wolpert, 1998). In the position control framework of myocontrol interfaces, target distance and speed are determined by the *EMG* magnitude, while the ability to contact small targets is determined by precision of the *EMG* signal, so in the context of signal dependent noise, precision decreases as magnitude increases (Fitts, 1954; Park et al., 2011). Therefore, for myocontrol, the speed-accuracy trade-off emerges from a mediation between the rate of muscle activation and its level of controllability (Park et al., 2017).

It has been shown that when subjects are asked to accurately control their myoelectric signals within a target, these signals behave in a manner compatible with the predictions of Fitts's law (Fimbel et al., 2006). Park et al. used Fitts's law to validate the suitability of *EMG* compared to force as a control source (Park et al., 2008; 2011). Williams and Kirsch used Fitts's law to evaluate head orientation and neck muscle *EMG* signals as control signals for patients with tetraplegia (Williams and Kirsch, 2009). Similarly, Choi et al. quantified the throughput for individuals with spinal cord injury when using myocontrol to move and click a cursor (Choi et al., 2013). Moreover, myocontrol is increasingly being used as human-computer interface for patient populations that may be affected by muscle weakness (Young et al., 2011a; Liyanagamage et al., 2017; Yang et al., 2018). However, these previous studies have not investigated how level of *EMG* activation affects performance independent of it is controllability. Fitts's law predicts that movement time is determined only by *ID*, which is determined entirely by the ratio between distance (*D*) and target width (*W*). Thus, it does not depend on absolute distance. However, it has been shown that Fitts's law breaks down as *ID* becomes small and very short distances are used in the task (Langolf et al., 1976; Gan and Hoffmann, 1988; Hoffmann, 2016). This suggests that controllability with myocontrol may be differently affected by ranges of *EMG* activation, which results with ranges of movement distance in the user interfaces. Thus, the aim of this study was to quantitatively assess how the range of target distances, namely the *EMG* activation, affects controllability in myocontrol in a Fitts's law task. Our hypothesis was that although accuracy increases at lower speeds, there would be a minimum level of noise present even at low levels of muscle activation, such that accuracy does not continue to improve at very low speed.

We asked subjects to control the vertical displacement of a cursor on a screen by contracting the first dorsal interosseous muscle (FDI). The movement distance covered by the cursor was proportional to the level of *EMG* activation of the FDI. We evaluated the speed-accuracy trade-off through the Fitts's task by manipulating movement distances (e.g. levels of *EMG* activation) and its accuracy demand (e.g. target width) to obtain five different *IDs* from a large range of distances. In particular, we were interested to investigate the effect of low levels of *EMG* activation on the controllability of myocontrol-based interfaces. We hypothesized that movement time is affected not only by the original formulation of Fitts's law due to the size of the target relative to the distance, but also by the target distance itself. We anticipated that low muscle activation to achieve short distance movements would result in a limited controllability due to higher variability and poor stabilization in reaching the target as required by the task demand.

2. Methods

2.1. Subjects

12 healthy subjects (mean 26 ± 4 years; 7 females) participated in this study. The University of Southern California Institutional Review Board approved all experimental procedures (UP-10–00,027). Subjects gave written informed consent. The experiment was performed in accordance with the Declaration of Helsinki and written authorization for use of protected health information was obtained and stored according to the Health Information Portability and Accountability Act.

2.2. Experimental setup

Participants sat on a chair and placed their dominant hand flat on the surface of a table with the palm down in a comfortable position. The index finger of the dominant hand was constrained to prevent abduction using a silicone block that adhered to the surface of the table. A surface *EMG* electrode (DE-2.3, Delsys Inc., MA, USA) with a band-pass filter of 20–450 Hz and an amplification of 1000 times was placed over the belly of the first dorsal interosseous (FDI). The *EMG* electrode signal was sampled at 1 kHz with an analog to digital interface (Power 1401, CED Technologies Inc., UK) and custom data acquisition software.

The isometric muscle activation signal for the experimental task was obtained by filtering the *EMG* signal from the electrode through three steps used by Young et al. (Young et al., 2011a). The signal was processed with a high-pass Butterworth filter (4th-order, 1 Hz cutoff), then a Bayesian filter, and finally a low-pass Butterworth filter (2nd-order, 5 Hz cutoff) to reduce jitter in the output signal. The Bayesian filter produces a smooth output that estimates the drive underlying the *EMG* signal, while also allowing fast low-latency changes in the filtered signal (Sanger, 2007). To ensure that the low-pass filter following the Bayesian filtered signal did not add significant delay to the myocontrol signal, pilot data on three subjects using the Bayesian filter alone obtained similar results to that presented in this paper.

Prior to the start of the experiment, the isometric maximal voluntary contraction (MVC) was measured from the FDI using the following procedure. The *EMG* signal was displayed as visual feedback for the

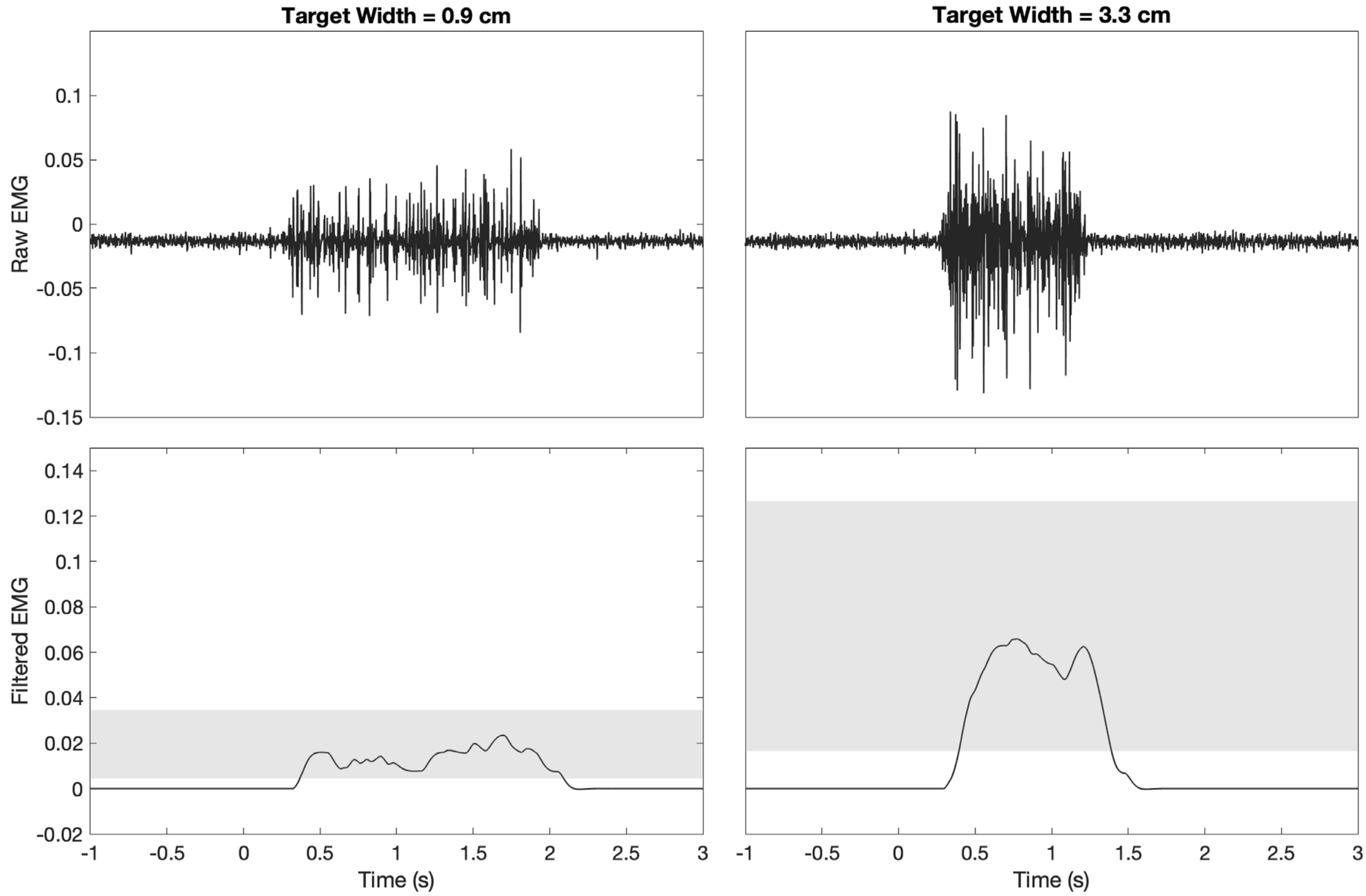

Fig. 1. Raw and filtered EMG signals from a subject for $ID = 1.38$ at width = 1.5 and 5.5. Shaded area represents the target region for each width condition.

participant via a horizontal bar target whose height on the screen represented the voltage level of the signal, thus stronger contractions moved the bar higher on the screen. The participant performed three attempts of 5 sec of maximum contraction for each muscle with encouragement and feedback. MVC was quantified by the data acquisition software as the maximum mean *EMG* activation measured over a 200 ms period. Following this measurement, all muscle activation levels for the experiment were expressed as normalized *EMG*, defined as the ratio of the *EMG* value of the muscle to its MVC.

2.3. Procedure

Each participant attended a single experimental session of approximately 1 hour duration. The session started with seating at the table, placement of the *EMG* electrode, and measurement of MVC. The participant then completed a series of trials during which they reached a target on a computer screen by activating their FDI.

During each trial, the *EMG* from the FDI controlled the vertical position of a cursor displayed on a monitor screen (37.5 cm width, 29.8 cm height, resolution 1280 × 1024 pixels) about 1 m from the subject's head. Vertical cursor position was linearly proportional to the *EMG* such that 0% MVC was the bottom of the screen and 50% MVC was the top of the screen, according to:

$$P = min\ (1,\ \ EMG(t)/(50\%MVC)) \tag{1}$$

where *P* is the position of the cursor between the bottom and the top of the monitor screen. The rate of cursor position was linearly proportional to the rate of filtered *EMG* signal. The cursor remained at the top of the screen for *EMG* values greater than 50% *MVC* and thus, feedback was effectively capped at 50% *MVC*. Prior to experimental trials, subjects were given two practice trials to practice moving the cursor on the screen and to ensure proper FDI activation.

Subjects were instructed to move the cursor from rest position into targets of different sizes as fast and accurately as possible. Prior to each target, subjects were asked to relax and keep the cursor at the bottom of the screen. As soon as the target appeared, subjects were instructed to reach the target as quickly as possible and maintain the position for 500 ms. The demand for subjects to stabilize in the target for 500 ms ensured that they maintained some control over the cursor, rather than inadvertently hiting the target or still adjusting the trajectory to achieve the accuracy demand (Dounskaia et al., 2005; Wisleder and Dounskaia, 2006; Fradet et al., 2008; Liyanagamage et al., 2017; Borish et al., 2018). Attempts where this 500 ms hold time was not accomplished within three seconds were considered unsuccessful in order to force the accomplishment of the task as quick as possible. Subjects had a three second rest period between targets to prevent fatigue. Subjects completed 10 blocks, reaching for 25 targets per block. Targets had varying Fitts's indices of difficulty (*ID*), measured in bits and calculated as

$$ID = log_2\left(\frac{2D}{W}\right) \tag{2}$$

Where, according to Fitts' s law, D was the movement distance from the bottom of the screen and the center of the target, and *W* was the width of the target (Fitts, 1954). Since the cursor position was proportional to the *EMG* activation from 0% to 50% of *MVC*, it is important to note that in our study the spatial definition of *D* and *W* resulted from the amount of *EMG* activation (as a fraction of *MVC*). Specifically, the 25 targets were divided into 5 different target width *W* conditions: 1.5, 2.5, 3.5, 4.5 and 5.5% of *MVC*, which resulted in 0.9, 1.5, 2.1, 2.7 and 3.3 cm target width on the screen respectively, and 5 different *IDs*: 1.38, 2.18, 2.83, 3.47, 4.06. These *IDs* were chosen to provide a large, yet feasible, range of difficulty. For each *ID* and *W*, the distance *D* was calculated based on Fitts' law, resulting in 25 different distances ranging from 2.0 to 45.8% of *MVC* (from 1.2 to 27.3 cm on screen). Thus distance values were: [1.2, 1.9, 2.7, 3.5, 4.3 cm], [2.0, 3.4, 4.7, 6.1, 7.4 cm], [3.2, 5.3, 7.4, 9.5, 11.7 cm], [5.0, 8.3, 11.6, 14.9, 18.2 cm], and [7.5, 12.4, 17.4, 22.4, 27.3 cm] for *IDs* 1.38, 2.18, 2.83, 3.47 and 4.06 respectively. For each width condition *W* there is a corresponding range of distances *D*, all with the same index of difficulty *ID*. For each block of trials, the 25 targets were presented in pseudo-random order. Fig. 1 shows example raw and filtered *EMG* signals from one subject for $ID = 1.38$ at the smallest and largest width conditions.

2.4. Analysis

Data analysis was executed with Matlab R2013a (Mathworks, Natick, MA). Statistical analysis was performed using RStudio, version 0.98.1056 (RStudio Inc., Boston, MA), and the R-package lme4, version 1.1–7.

2.4.1. Cursor analysis

With Fitts's law, only successful trials are used to regress movement time with *ID* (Fitts, 1954). In order to correlate other outcome measures with observations from the movement time regression, only successful trials were used for analysis. The start of the cursor movement was defined as the time when the cursor velocity was at least 5% of the peak velocity observed during the trial, similar to previous studies (Bertucco and Cesari, 2010; Bertucco et al., 2013). The end of the movement was at the end of the 500 ms hold inside the target. Movement time (*MT*) was defined as the time from the movement start to movement finish.

Cursor velocity and acceleration were derived from the cursor position. From the cursor velocity, the reaching phase of the movement was determined. Reaching phase was defined as the time from movement start to when the velocity first crosses zero. The position at the velocity zero-crossing was used to calculate the overshoot or undershoot of the cursor normalized to the target distance (*D*) as:

$$\text{overshoot / undershoot} = \frac{x\text{–nearest target boundary}}{D} \tag{3}$$

where *x* is the cursor position.

Acceleration time was defined as the time from movement start to the time of peak velocity observed prior to the 500 ms hold.

Standard deviation (STD) and coefficient of variation (CV) of the cursor position were also calculated for each trial. STD of the cursor position was calculated from the end of the reaching phase to the beginning of the hold, which was defined as the stabilization phase. CV was calculated as the ratio between STD of the cursor position and the mean of the cursor position during the stabilization phase.

2.4.2. Statistical analysis

Statistical analysis was performed using RStudio (RStudio Inc., Version 0.98.109, Boston, MA). In order to test Fitts's Law, linear regressions were performed by the method of least squares for the averaged *MT* values across subjects. The correlation coefficient was used to indicate the goodness of fit of *MT* as a function of *ID* (Fitts, 1954). We performed a linear mixed effects model (*lmer* function, R-package 'lme4') on the following dependent variables: movement time, success, overshoot/undershoot, acceleration time, STD and CV. As fixed effects, we entered *ID* ((5 levels) and Width (5 levels) into the model. As random effects, and intercepts for each subject as a random effect. Thus, the model was given by:

$$Dependent variable \sim Width + ID + (1|Subject) \tag{4}$$

Once the models were created, we compared the model including all the factors (Full) against a reduced model without the effect in question (Null) in order to test if the fixed effects significantly affected the dependent variable. In order to test interaction between the two fixed effects (*ID* and Width), we compared the model that takes into account the interaction between fixed effects (Full) against the model without the interaction (Null). For all comparisons, we used likelihood ratio test as a means to attain p-values and Akaike's information criterion values (AIC) (Akaike, 1992). Likelihood is the probability of seeing the data given a model. The logic of the likelihood ratio test is to compare the likelihood of two models with each other. We performed the likelihood ratio test using ANOVA (*anova* in R) to compare the two models. If the factor in question significantly affects the dependent variable, then the comparison with ANOVA will report a significant *p*-value (<0.05) and an AIC value lower for the Full model. Similarly, a significant interaction between factors will result in a significant difference between the Full and the Null models ($p < 0.05$) with a lower AIC for the Full model. Pairwise *t*-test with Bonferroni adjustment was used for post-hoc analysis to identify at which *IDs* there was a significant difference across width conditions.

3. Results

3.1. Movement time

Speed-accuracy trade-off is typically evaluated by the robustness of the linear relationship between *MT* and *ID* as described by the Fitts's law formulation (Fitts, 1954). A departure from such correlation between these two parameters signifies a weakening of the mediation between speed and accuracy.

In our study, *MT* showed a significant linear regression on ID for all the target widths ($p < 0.01$) except for the 0.9 cm target ($p = 0.098$). The correlation coefficients ranged from 0.980 to 0.994 for $W = 1.5$, 2.1 2.7 and 3.3 cm, whereas it showed a departure from linear relationship for the $W = 0.9$ cm resulting with a correlation coefficient equal to 0.807. Interestingly, when using a cubic polynomial regression fitting the norm of residuals resulted in one sixth the variance (0.0305) with respect to the residuals with linear fitting (0.1815) for $W = 0.9$ cm, although this may have been explained by the larger number of parameters in the cubic fit.

Results from the likelihood ratio test on *MT* are shown in Table 1.

Table 1
Likelihood ratio results.

	Factor	AIC_{Full}	AIC_{Null}	*p*-value
Movement time	*ID*	4131.3	5289.3	< 0.0001
	Width	4131.3	4377.3	< 0.0001
	*ID**Width	4087.3	4131.3	< 0.0001
Success	*ID*	−288.10	−203.16	< 0.0001
	Width	−288.10	−189.75	< 0.0001
	*ID**Width	−294.49	−288.10	0.004
Overshoot/undershoot	*ID*	−3002.5	−2824.0	< 0.0001
	Width	−3002.5	−2984.2	< 0.0001
	*ID**Width	−3096.1	−3002.5	< 0.0001
Acceleration	*ID*	−3135.9	−3003.7	< 0.0001
	Width	−3135.9	−3127.9	0.002
	*ID**Width	−3218.4	−3135.9	< 0.0001
STD	*ID*	−26,890	−26,501	< 0.0001
	Width	−26,890	−26,864	< 0.0001
	*ID**Width	−26,900	−3135.9	< 0.001
CV	*ID*	−8494.4	−8334.1	< 0.0001
	Width	−8494.4	−7769.8	< 0.0001
	*ID**Width	−8682.2	−8494.4	< 0.0001

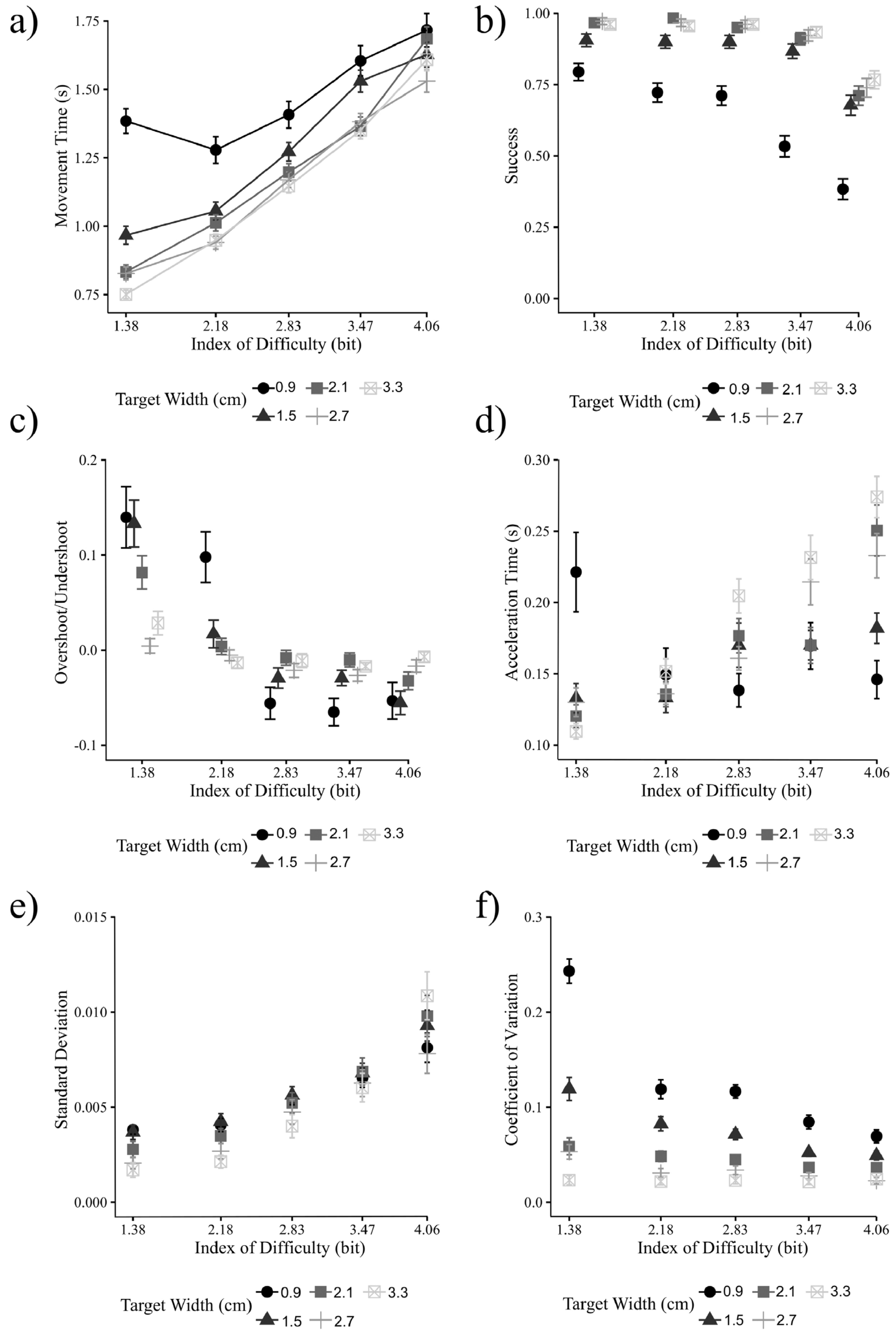

Fig. 2. (a) *MT* of successful trials across *IDs* and width conditions. There is a significant increase in *MT* at the lower *IDs* for the smallest target width condition. (b) Proportion of successful trials across *ID* and width condition. There was lower success for the smallest width condition. (c) Overshoot (>0) or undershoot (<0) across *IDs* and width conditions. At low *IDs*, there was more overshoot for the smaller width targets. (d) Acceleration time across *IDs* and width conditions. At low *IDs*, the acceleration time was significantly longer for $W = 0.9$ cm than for the rest of the width conditions. (e) STD of the cursor position during the stabilization phase across *IDs* and width conditions. There is increasing signal-dependent noise in all width conditions, but the increase is greater in the larger width targets. (f) CV of cursor position during the stabilization phase across *IDs* and widths conditions. There is a larger decrease in coefficient of variation for the smaller width targets.

Table 1 shows the AIC values for the Null and Full models, and the *p*-value for the comparison between the two models using ANOVA for each factor and their interaction. The likelihood ratio test showed that *ID* had a significant effect on *MT*, meaning that the task effectively imposed a speed-accuracy trade-off. On average, *MT* was 0.957 (95% CI [0.878, 1.036]), 1.053 (95% CI [0.974, 1.132]), 1.246 (95% CI [1.166, 1.325]), 1.459 (95% CI [1.380, 1.539]) and 1.657 sec (95% CI [1.576, 1.738]) for *ID* 1.38, 2.18, 2.83, 3.47 and 4.06 respectively. *MT* increased with *ID* by 0.27 $\pm$ 0.01 sec/bit. Target width also had a significant effect on *MT*, with *MT* decreasing with width by 0.132 $\pm$ 0.008 sec/cm. The likelihood ratio test showed that the interaction between target width and *ID* had a significant effect on the movement time, meaning the effect of *ID* on *MT* was different for the different width conditions. As shown in Fig. 2a at higher width conditions, movement time followed a Fitts's law behavior, increasing linearly with *ID* with similar slope. However, for $W = 0.9$ cm, movement time increased at the lower *IDs* corresponding to lower target distances. Indeed, the increased movement time at lower *IDs* deviates from our predictions based on Fitts's law. Movement time for $W = 0.9$ cm was significantly longer than the time for all other target widths at $ID = 1.38$ ($p < 0.0001$) and $ID = 2.18$ ($p < 0.005$). It was longer than the time for the three largest widths at $ID = 2.83$ ($p < 0.01$) and $ID = 3.47$ ($p < 0.02$). Movement time for $W = 1.5$ cm was significantly longer than the time for $W = 3.3$ cm at $ID = 1.38$ ($p < 0.001$) and $ID = 3.47$($p = 0.04$). At the highest *ID*, there was no significant difference between width conditions for movement time.

3.2. Success

On average, success was 0.92 (95% CI [0.87, 0.97]), 0.91 (95% CI [0.86, 0.95]), 0.90 (95% CI [0.85, 0.95]), 0.83 (95% CI [0.78, 0.88]) and 0.66 (95% CI [0.61, 0.70]) for ID 1.38, 2.18, 2.83, 3.47 and 4.06 respectively. The likelihood ratio test showed that *ID* had a significant effect on success (Table 1). Success decreased with *ID* by 0.087 $\pm$ 0.009 per bit. Target width also had a significant effect on success, with success increasing with width by 0.107 $\pm$ 0.010 per cm. The likelihood ratio test showed that the interaction between target width and *ID* had a significant effect on success, meaning the effect of *ID* on success was different for the different width conditions. Post- hoc analysis showed that success for $W = 0.9$ cm was significantly lower than the highest three widths at $ID = 2.18$ ($p < 0.01$) and 2.83 ($p < 0.01$). Success for $W = 0.9$ cm was lower for all other widths at $ID = 3.47$ ($p < 0.0001$) and 4.06 ($p < 0.0001$) (Fig. 2b).

3.3. Overshoot/undershoot

Results from the likelihood ratio test on success are shown in Table 1. The likelihood ratio test showed that *ID* had a significant effect on overshoot or undershoot. On average, overshoot or undershoot was 0.079 (95% CI [0.053, 0.106]), 0.021 (95% CI [−0.006, 0.047]), −0.023 (95% CI [−0.050, 0.003]), −0.026 (95% CI [−0.053, 0.001]) and −0.028 (95% CI [−0.056, −0.001]) for ID 1.38, 2.18, 2.83, 3.47 and 4.06 respectively. Overshoot or undershoot decreased with *ID* by -0.039 $\pm$ 0.003 per bit. Target width also had a significant effect on overshoot or undershoot, decreasing with width by 0.0145 $\pm$ 0.003 per cm. The likelihood ratio test showed that the interaction between target width and *ID* had a significant effect on the overshoot or undershoot, meaning the effect of *ID* on overshoot or undershoot was different for the different width conditions. At $ID = 1.38$, subjects had a significant overshoot for $W = 0.9$ cm compared to $W = 2.7$ cm ($p < 0.0001$) and $W = 3.3$ cm ($p < 0.0001$). Subjects also had significant overshoot for $W = 1.5$ cm compared to $W = 2.7$ cm ($p < 0.001$) and $W = 3.3$ cm ($p < 0.001$). There was also a significant difference between $W = 2.1$ cm and $W = 2.7$ cm ($p = 0.003$). At $ID = 2.18$, subjects had more overshoot for $W = 0.9$ cm compared to all other widths ($p < 0.01$) (Fig. 2c).

3.4. Acceleration time

The likelihood ratio test showed that *ID* had a significant effect on acceleration time (Table 1). On average, acceleration time was 0.143 (95% CI [0.118, 0.168]), 0.142 (95% CI [0.117, 0.167]), 0.170 (95% CI [0.145, 0.195]), 0.192 (95% CI [0.167, 0.218]) and 0.220 sec (95% CI [0.194, 0.246]) for ID 1.38, 2.18, 2.83, 3.47 and 4.06 respectively. Acceleration time increased with ID by 0.033 $\pm$ 0.003 sec/bit. Target width also had a significant effect on acceleration time, increasing with width by 0.01 $\pm$ 0.003 003 sec/cm. The likelihood ratio test showed that the interaction between target width and *ID* had a significant effect on the acceleration time, meaning the effect of *ID* on acceleration time was different for the different width conditions. At $ID = 1.38$, the acceleration time for $W = 0.9$ cm was significantly greater than the time for all other width conditions ($p < 0.001$). At $ID = 4.06$, the acceleration time for $W = 0.9$ cm was significantly shorter than the time for $W = 2.1$ cm ($p = 0.004$) and $W = 3.3$ cm ($p < 0.0001$). It was also significantly shorter for $W = 1.5$ cm than for $W = 3.3$ cm (Fig. 2d).

3.5. Standard deviation and coefficient of variation

On average, STD was 0.003 (95% CI [0.001, 0.005]), 0.003 (95% CI [0.002, 0.005]), 0.005 (95% CI [0.003, 0.007]), 0.007 (95% CI [0.005, 0.009]) and 0.010 (95% CI [0.008, 0.012]) for ID 1.38, 2.18, 2.83, 3.47 and 4.06 respectively. The likelihood ratio test showed that ID had a significant effect on STD (Table 1). On average, STD increased with *ID* by 0.0025 $\pm$ 0.0001 per bit. Target width also had a significant effect on STD, decreasing with width by 0.00072 $\pm$ 0.00001 per cm. There was significant interaction between target width and ID on STD (Fig. 2e).

On average, CV was 0.10 (95% CI [0.08, 0.12]), 0.06 (95% CI [0.04, 0.08]), 0.06 (95% CI [0.04, 0.08]), 0.05 (95% CI [0.03, 0.07]) and 0.05 (95% CI [0.03, 0.06]) for ID 1.38, 2.18, 2.83, 3.47 and 4.06 respectively. Results from the likelihood ratio test on success are shown in Table 1. The likelihood ratio test showed that *ID* had a significant effect on CV. On average, CV decreased with *ID* by 0.018 $\pm$ 0.001 per bit. Target width also had a significant effect on CV, decreasing with width by 0.043 $\pm$ 0.002 per cm. There was significant interaction between target width and *ID* on CV (Fig. 2f).

4. Discussion

The purpose of this study was to investigate how level of muscle activation affects the controllability in myocontrol using Bayesian-filtered *EMG*. To the authors' knowledge, this is the first study to observe how the speed-accuracy tradeoff in myocontrol changes as a result of varying ranges of distances, that is *EMG* activation itself. Subjects had less success reaching targets of the lowest range of distances. Additionally, low distance targets resulted in longer movement time, more overshoot, and longer acceleration time at the low *ID*. These results suggest that movement time in myocontrol is affected not only by the classical Fitts's law relationship (Fitts, 1954), but also by target distance, namely *EMG* activation. Small distances paired with high accuracy demand actually increased the difficulty for subjects to reach the target. The longer acceleration time may indicate some pre-planning of the movement in anticipation of the target's perceived difficulty. The overshoot suggests that subjects are unable to initially reach the target at such a small distance.

According to Fitts's law, movement time should be a linear function of *ID*. However, certain width conditions at smaller *IDs* exhibited a disproportionate increase in movement time, thus deviating from Fitts's law. Sheridan noted previously that a reduction in target width resulted in a higher increase in movement time compared to a similar increase in distance in Fitts's law (Sheridan, 1979). In an experiment in which subjects tapped between two targets with a pen, it was shown that when speed was related to the distribution of movement endpoints instead of the actual target widths, authors observed a departure from the linear relationship predicted by Fitts's law (Welford et al., 1969). A study in rapid wrist rotations also observed significant effects of target width within *ID* levels, such that authors proposed an adjusted speed-accuracy trade-off linear relationship where target distance and width parameters were independently considered in the mathematical formulation (Meyer et al., 1988). These previous studies suggest that the observed increase in movement time at small width conditions at lower *IDs* is a biological property that is not predicted by Fitts's law, and not unique to myocontrol.

Previous studies have tested myocontrol on the Fitts's law model using similar paradigms. In a myocontrol task using biceps and triceps muscles it was found that movement time to reach a target could be modeled using Fitts' law (Park et al., 2011). However, the authors used movement distances that ranged from 15% to 100% of *MVC*. Instead, in our study *IDs* and target widths were manipulated to obtain movement distances with lower levels of *EMG* activation, such that only 9 out of 25 experimental conditions resulted with *EMG* activation higher than 15% of *MVC*. This further suggests that linearity of Fitts's law in myocontrol depends on the selection of ranges *EMG* activation in the *ID* calculation. In an earlier study Fitts's law was tested using myoelectric signal from hand and forehead muscles with a range of *EMG* activations in which the shortest distance, resulting with the smallest *ID*, corresponded to 6.25% *MVC* (Fimbel et al., 2006). Interestingly, it was found an unexpected inverted-U pattern for the movement time on *IDs*, which was analogous to the departure from the linearity we found for the $W = 0.9$ cm condition. Nonetheless, the authors did not test different combinations of movement distances (e.g. *EMG* activations) and targets width across the same smallest *ID*, thus it was not possible to demonstrate whether the cause of the concave pattern was due to the limited controllability with low levels of muscle activation or based on the user interface itself.

The task demand for subjects to hit low distance, high accuracy targets as quickly and accurately as possible may actually contradict what they are capable of accomplishing physiologically. It is possible that at very low distances, subjects are primarily recruiting smaller motor units. Milner-Brown et al. found that motor units in the FDI are recruited in accordance to the size of contraction they produce as subjects maintained a force at the threshold for steady motor unit recruitment, thus following Henneman's size principle (Milner-Brown et al., 1973b). In another study, Milner-Brown et al. had subjects perform a force tracking task with the FDI. At low force levels, they found that recruitment of additional motor units is the major mechanism for increasing the force of voluntary contraction (Milner-Brown et al., 1973a).

The decreased number of motor unit recruitment also describes the observed increase in CV at lower *IDs*, which is consistent with literature that observed increased CV at lower force levels (Galganski et al., 1993; Enoka et al., 1999; Laidlaw et al., 2000; Moritz, 2005; Taylor, 2003; Jones et al., 2002; de C. Hamilton et al., 2004). Thus, signal-dependent noise is not proportional to force levels below a certain threshold for the FDI. This has been observed in previous work on the FDI. In a study looking at effects of age on motor output from the FDI, SD increased with target force level, while CV decreased with relative target level for both young and elderly subjects (Galganski et al., 1993; Enoka et al., 1999). Laidlaw et al. found similar results in a study comparing steadiness of the FDI in young and elderly subjects (Laidlaw et al., 2000). Simulations of force produced by a pool of motor units with characteristics resembling those of the FDI suggest that higher variability at low forces may result from increased discharge rate variability, and such variability decreases exponentially with increasing force in the FDI (Moritz, 2005). This effect may also be due to synchronization and low-frequency common oscillation of motor units (Taylor, 2003). Results of another motor-unit pool model suggest that the orderly recruitment of motor neurons contributes to linearly increasing signal dependent noise and a higher CV at lower forces (Jones et al., 2002). This behavior may not be limited to the FDI. Simulations of strong and weak muscles suggest that both have a higher CV in the bottom 5% of the force range as a result of the number of motor units being recruited (de C. Hamilton et al., 2004). This is in accordance with our findings where we found a departure from the Fitts's law relationship and significantly higher CV in task conditions with the level of muscle activations below 5% of *MVC*. Yet, these conditions were characterized by low accuracy demand (e.g. small *IDs*), suggesting that poor cursor controllability is mainly attributable to increased variability of motor firing at low levels of force (Moritz, 2005). Additional studies with a larger cohort of subjects would be needed to quantify an optimal range and its variance of this critical threshold of muscle activation that leads to poor controllability of cursor position for single-muscle myocontrol.

Our study was run in only one session, thus we did not test the effects of practice on learning the controllability of the cursor. Recent studies have shown that speed-accuracy trade-off improves with practice (Shmuelof et al., 2012) and neuromotor noise is reduced in long-term motor skill learning (Huber et al., 2016). Further studies are needed to investigate the effect of practice with myocontrol interfaces on the speed-accuracy trade-off function, and whether learning can attenuate the limited control at low levels of muscle activation.

Force was not measured, however, literature suggests that isometric *EMG* is a good estimate of force (Milner-Brown and Stein, 1975). Moreover, the focus of this study was on what subjects were able to accomplish with myoelectric signals, so force measurements were unnecessary to the goal of our study.

There are possible limitations to this study. It is possible that the behavior observed at small distances is a result of the filter. There are fewer spikes at lower distances, which results in a noisier output in the nonlinear filter, making it difficult to stabilize in the targets with small width. It may be possible that the output could be smoothed by changing the Bayesian filter parameters or using different non-linear control algorithms for the *EMG* signal (Karlik et al., 2003; Chan and Englehart, 2005; Liu et al., 2007;). More studies would be required to verify this.

In order to truly explain what might be happening at the motoneuron level, intramuscular *EMG* would be more informative, as *EMG* may not be the best indicator to explain what is happening (Farina et al., 2002; Farina, 2004).

Despite the limitations of our study, our results clearly show that there exists a minimal threshold of target distance and width for fast and accurate myoelectric control. This is important to know when implementing myocontrol clinically. Naturally, myocontrol applications want to use low levels of muscle activation to avoid fatigue and reduce signal-dependent-noise. However, there exists a lower threshold that may either be due to physiological limitations or filtering limitations. Thus, there is a need to pay attention to the amount of muscle activation to optimize controllability of myocontrol interfaces. For some pathological situations, myocontrol may be used as a rehabilitative tool (Young et al., 2011b). In this case, patients should use their optimal range to receive appropriate feedback on their muscle activations. For myocontrolled devices, users should be calibrated to operate the device within an activation range that allows them the highest bandwidth possible for fast and accurate control. In general, controllability of myocontrolled devices should be facilitated as much as possible. Thus, myocontrol applications should require control signals with sufficient recruitment to reduce the variability at low forces, but not such high recruitment that subjects become fatigued. Future work may focus on modifying other filter properties such as delay, gain, or frequency components to further improve myocontrol controllability.

CRediT authorship contribution statement

Cassie N. Borish: Conceptualization, Data curation, Formal analysis, Writing - original draft. **Matteo Bertucco:** Conceptualization, Formal analysis, Writing - review & editing. **Terence D. Sanger:**

Conceptualization, Writing - review & editing.

Declaration of Competing Interest

The authors declared no potential conflicts of interest with respect to the research, authorship, and/or publication of this article.

Acknowledgment

The authors would like to thank Adam Feinman for his contributions to this study. This research was supported by the Don and Linda Carter Foundation, the Crowley-Carter Foundation and the Department of Biomedical Engineering, University of Southern California.

References

Akaike, H., 1992. Information theory and an extension of the maximum likelihood principle. in: breakthroughs in statistics. In: Kotz, S., Johnson, NL (Eds.), Springer Series in Statistics (Perspectives in Statistics). Springer, New York, NY, pp. 610–624.
Ambrosini, E., Ferrante, S., Schauer, T., Klauer, C., Gaffuri, M., Ferrigno, G., Pedrocchi, A., 2014. A myocontrolled neuroprosthesis integrated with a passive exoskeleton to support upper limb activities. J. Electromyogr. Kinesiol. 24 (2), 307–317.
Bertucco, M., Cesari, P., 2010. Does movement planning follow Fitts' law? Scaling anticipatory postural adjustments with movement speed and accuracy. Neuroscience 171 (1), 205–213.
Bertucco, M., Cesari, P., Latash, M., 2013. Fitts law in early postural adjustments. Neuroscience 231, 61–69.
Bloom, R., Przekop, A., Sanger, T.D., 2010. Prolonged electromyogram biofeedback improves upper extremity function in children with cerebral palsy. J. Child. Neurol. 25 (12), 1480–1484.
Borish, C.N., Feinman, A., Bertucco, M., Ramsy, N.G., Sanger, T.D., 2018. Comparison of speed-accuracy tradeoff between linear and nonlinear filtering algorithms for myocontrol. J. Neurophysiol 119, 2030–2035.
Chan, A.D., Englehart, K.B., 2005. Continuous myoelectric control for powered prostheses using hidden Markov models. IEEE Trans. Biomed. Eng. 52, 121–124.
Childress, D.S., 1985. Historical aspects of powered limb prostheses. Clin. Prosthet. Orthot. 9 (1), 2–13.
Choi, C., Na, Y., Rim, B., Kim, Y., Kang, S., Kim, J., 2013. An SEMG computer interface using three myoelectric sites for proportional two- dimensional cursor motion control and clicking for individuals with spinal cord injuries. Med. Eng. Phys. 35 (6), 777–783.
de C. Hamilton, A.F., Jones, K.E., Wolpert, D.M., 2004. The scaling of motor noise with muscle strength and motor unit number in humans. Exp. Brain. Res. 157 (4), 417–430.
Dounskaia, N., Wisleder, D., Johnson, T., 2005. Influence of biomechanical factors on substructure of pointing movements. Exp. Brain. Res. 164, 505–516.
Enoka, R.M., Graves, A.E., Kornatz, K.W., Laidlaw, D.H., 1999. Task- and age-dependent variations in steadiness. Progr. Brain. Res. 123, 389–395.
Farina, D., 2004. The extraction of neural strategies from the surface EMG. J. Appl. Physiol. 96 (4), 1486–1495.
Farina, D., Fosci, M., Merletti, R., 2002. Motor unit recruitment strategies investigated by surface EMG variables. J. Appl. Physiol. 92, 235–247.
Farina, D., Amsuss, S., 2016. Reflections on the present and future of upper limb prostheses. Expert Rev. Med. Devices 13, 321–324.
Fimbel, E.J., Lemay, M., Arguin, M., 2006. Speed accuracy trade-offs in myocontrol. Hum. Mov. Sci. 25 (2), 165–180.
Fitts, P.M., 1954. The information capacity of the human motor system in controlling the amplitude of movement. J. Exp. Psychol. 47 (6), 381–390.
Fradet, L., Lee, G., Dounskaia, N., 2008. Origins of submovements during pointing movements. Acta Psychol. (Amst). 129, 91–100.
Galganski, M.E., Fuglevand, A.J., Enoka, R.M., 1993. Reduced control of motor output in a human hand muscle of elderly subjects during submaximal contractions. J. Neurophysiol. 69 (6), 2108–2115.
Gan, K.-C., Hoffmann, E.R., 1988. Geometrical conditions for ballistic and visually controlled movements. Ergonomics 31, 829–839.
Gusman, J., Mastinu, E., Ortiz-Catalan, M., 2017. Evaluation of computer-based target achievement tests for myoelectric control. IEEE J. Transl. Eng. Heal. Med. 5, 2100310.
Hoffmann, E.R., 2016. Critical index of difficulty for different body motions: a review. J. Mot. Behav. 48, 277–288.
Hofmann, D., Jiang, N., Vujaklija, I., Farina, D., 2016. Bayesian filtering of surface EMG for accurate simultaneous and proportional prosthetic control. IEEE Trans. Neural. Syst. Rehabil. Eng. 24 (12), 1333–1341.
Huber, M.E., Kuznetsov, N., Sternad, D., 2016. Persistence of reduced neuromotor noise in long-term motor skill learning. J. Neurophysiol. 116, 2922–2935.
Jones, K.E., Hamilton, A.F., Wolpert, D.M., 2002. Sources of signal-dependent noise during isometric force production. J. Neurophysiol. 88 (3), 1533–1544.
Kamavuako, E.N., Scheme, E.J., Englehart, K.B., 2014. On the usability of intramuscular EMG for prosthetic control: a Fitt's law approach. J. Electromyogr. Kinesiol. 24, 770–777.
Karlik, B., Tokhi, M.O., Alci, M.A., 2003. Fuzzy clustering neural network architecture for multifunction upper-limb prosthesis. IEEE Trans. Biomed. Eng. 50, 1255–1261.
Laidlaw, D.H., Bilodeau, M., Enoka, R.M., 2000. Steadiness is reduced and motor unit discharge is more variable in old adults. Muscle Nerve 23, 600–612.
Langolf, G.D., Chaffin, D.B., Foulke, J.A., 1976. An investigation of Fitts' law using a wide range of movement amplitudes. J. Mot. Behav. 8, 113–128.
Liyanagamage, S.A., Bertucco, M., Bhanpuri, N.H., Sanger, T.D., 2017. Scaled vibratory feedback can bias muscle use in children with dystonia during a redundant, 1-Dimensional myocontrol task. J. Child. Neurol. 32, 161–169.
Liu, Y.-.H., Huang, H.-.P., Weng, C.-.H., 2007. Recognition of electromyographic signals using cascaded kernel learning machine. IEEE/ASME Trans. Mechatron. 12, 253–264.
MacKenzie, I.S., 1992. Fitts' law as a research and design tool in human- computer interaction. Hum. Comput. Interact. 7 (1), 91–139.
Meyer, D.E., Abrams, R.A., Kornblum, S., Wright, C.E., Keith Smith, J.E., 1988. Optimality in human motor performance: ideal control of rapid aimed movements. Psychol. Rev. 95 (3), 340.
Milner-Brown, H.S., Stein, R.B., 1975. The relation between the surface electromyogram and muscular force. J. Physiol. 246 (3), 549–569.
Milner-Brown, H.S., Stein, R.B., Yemm, R., 1973a. Changes in firing rate of human motor units during linearly changing voluntary contractions. J. Physiol. 230 (2), 371–390.
Milner-Brown, H.S., Stein, R.B., Yemm, R., 1973b. The orderly recruitment of human motor units during voluntary isometric contractions. J. Physiol. 230 (2), 359–370.
Moritz, C.T., 2005. Discharge rate variability influences the variation in force fluctuations across the working range of a hand muscle. J. Neurophysiol. 93 (5), 2449–2459.
Niu, C.M., Lee, K., Houde, J.F., Sanger, T.D., 2015. Vowel generation for children with cerebral palsy using myocontrol of a speech synthesizer. Front. Hum. Neurosci. 8, 1077.
Park, J., Bae, W., Kim, H., Park, S., 2008. EMG force correlation considering Fitts law. In: Proceeding of IEEE International Conference On Multisensor Fusion and Integration for Intelligent Systems. MIF, pp. 644–649 2008.
Park, J., Kim, H., Chung, W., Park, S, 2011. Comparison of myocontrol and force control based on fitts' law model. Int. J. Precis. Eng. Manuf 12, 211–217.
Plamondon, P., Alimi, A.M., 1997. Speed/accuracy trade-offs in target-directed movements. Behav. Brain. Sci. 20, 279–349.
Sanger, T.D., 2007. Bayesian filtering of myoelectric signals. J. Neurophysiol. 97 (2), 1839–1845.
Scheme, E.J., Englehart, K.B., 2013. Validation of a selective ensemble-based classification scheme for myoelectric control using a three-dimensional Fitts' law test. IEEE Trans. Neural. Syst. Rehabil. Eng. 21, 616–623.
Seifert, H.M., Fuglevand, A.J., 2002. Restoration of movement using functional electrical stimulation and Bayes' theorem. J. Neurosci. 22 (21), 9465–9474.
Shannon, C.E., 1948. A mathematical theory of communication. Bell Syst. Tech. J. 27 (3), 379–423.
Sheridan, M.R., 1979. A reappraisal of Fitts law. J. Mot. Behav. 11 (3), 179–188.
Shmuelof, L., Krakauer, J.W., Mazzoni, P., 2012. How is a motor skill learned? Change and invariance at the levels of task success and trajectory control. J. Neurophysiol 108, 578–594.
Smith, L.H., Kuiken, T.A., Hargrove, L.J., 2016. Evaluation of linear regression simultaneous myoelectric control using intramuscular EMG. IEEE Trans. Biomed. Eng. 63, 737–746.
Soukoreff, R., MacKenzie, I., 2004. Towards a standard for pointing device evaluation, perspectives on 27 years of Fitt's law research in HCI. Int. J. Hum. Comput. Stud. 61, 751–789.
Staudenmann, D., Roeleveld, K., Stegeman, D.F., van Dien, J.H., 2010. Methodological aspects of SEMG recordings for force estimation a tutorial and review. J. Electromyogr. Kinesiol. 20 (3), 375–387.
Taylor, A.M., 2003. Multiple features of motor-unit activity influence force fluctuations during isometric contractions. J. Neurophysiol. 90 (2), 1350–1361.
Vujaklija, I., Shalchyan, V., Kamavuako, E.N., Jiang, N., Marateb, H.R., Farina, D., 2018. Online mapping of EMG signals into kinematics by autoencoding. J. Neuroeng. Rehabil. 15, 21.
Welford, A.T., Norris, A.H., Shock, N.W., 1969. Speed and accuracy of movement and their changes with age. Acta Psychol 30, 3–15.
Williams, M.R., Kirsch, R., 2009. Evaluation of 2d and 3d command sources for individuals with high tetraplegia. IEEE Trans. Neural. Syst. Rehabil. Eng. 16 (5), 485–496.
Wisleder, D., Dounskaia, N., 2006. The role of different submovement types during pointing to a target. Exp. Brain. Res. 176, 132–149.
Yang, C., Long, J., Urbin, M.A., Feng, Y., Song, G., Weng, J., Li, Z., 2018. Real-Time myocontrol of a human–computer interface by paretic muscles after stroke. IEEE Trans. Cogn. Dev. Syst. 10, 1126–1132.
Young, S.J., Bertucco, M., Sanger, T.D., 2014. Cathodal transcranial direct current stimulation in children with dystonia: a sham-controlled study. J. Child. Neurol. 29 (2), 232–239.
Young, S.J., van Doornik, J., Sanger, T.D., 2011a. Finger muscle control in children with dystonia: children with dystonia. Mov. Disord. 26 (7), 1290–1296.
Young, S.J., van Doornik, J., Sanger, T.D., 2011b. Visual feedback reduces co-contraction in children with dystonia. J. Child. Neurol. 26 (1), 37–43.